Comparison of One- and Two-day Protocols for Myocardial SPET: A Monte Carlo Study

H. H. El-Ali, MSc[1], John Palmer, PhD[1], Marcus Carlsson, MD[2], Lars Edenbrandt, PhD[3], Michael Ljungberg, PhD[1]

[1]Department of Medical Radiation Physics, The Jubileum Institution, Lund University, Sweden
[2]Department of Clinical Physiology, Lund University Hospital, Sweden
[3]Department of Clinical Physiology, Malmoe University Hospital, Sweden

---

Correspondence should be sent to:
H. H. El-Ali, MSc
Department of Medical Radiation Physics
The Jubileum Institute,
Lund University
SE-221 85 Lund, SWEDEN
Phone: +46 46 178543
Fax: +46 46 178540
Email: Henrik_hussein.el_ali@radfys.lu.se

Keywords: Cardiac, Quantification, SPET, Perfusion, Monte Carlo

Abstract

Myocardial perfusion single-photon emission tomography (SPET) is carried out by combining a rest and a stress study that are performed either on one day or two separate days. A problem when performing the two studies on one day is that the residual activity from the first study contributes to the activity measured in the second study. Our aim was to evaluate how the quantification of myocardial perfusion images is influenced by different types of one- and two-day rest-stress protocols.

Methods: A digital phantom was used for the generation of heart images and a Monte Carlo based scintillation camera program was used to simulate SPET projection images. In our simulations, the rest images were normal and the stress images included lesions of different type and localisation. Two programs for quantification of myocardial perfusion images were used to assess the different images in an automated and objective way.

Results: The summed difference scores observed with the two-day protocol were 3 ± 1 (mean ± SD) higher for AutoQUANT and 2 ± 1 higher for 4D-MSPECT compared to those observed with the one-day protocol. The extent values were 2 percentage points higher for the two-day protocol compared to the one-day protocol for both programs.

Conclusions: There are differences in the quantitative assessment of perfusion defects depending on the type of protocol used. The contribution of residual activity is larger when a one-day protocol is used and if a high dose is given at the first examination. The differences could have clinical consequences and result in incorrect image interpretations.

Introduction

Myocardial perfusion scintigraphy with single-photon emission tomography (SPET) is a method that is widely used to assess ischaemic heart diseases (1). Such investigations are carried out by combining a rest study and a stress study that are performed either on the same day or on two separate days (2-5). A one-day protocol can be performed either as a stress-rest or a rest-stress combination. Performing a complete study on a single day is of advantage logistically, as well as providing better communication between the patient and the staff. A known potential problem when performing two studies on the same day is that the residual activity from the first study contributes to the activity measured in the second study (2). In order to minimize the effect of this unwanted contribution, a larger amount of activity must be administered to the patient during the second study. The relationship between the activities administered in the two studies is often 300:900 MBq and the total amount is limited by national regulations. This means that there is a trade-off between the image quality in terms of a high signal-to-noise ratio in the first study and the unwanted contribution from the residual activity from this study in the second study. Clinical studies support the usefulness of both one-day and two-day protocols (2-4;6), but a detailed comparison of these protocols has, to our knowledge, not been performed previously.

The European Union requires member states to promote the establishment and use of Diagnostic Reference Levels (DRLs) (7), which limit the administered activity for nuclear and radiological examinations. Derived Swedish national regulations assign a DRL of 1200 MBq for a complete rest/stress study, regardless of the type of protocol. In obese patients, a significant amount of the emitted photons is attenuated, and a relatively high dose must be administered for the rest study in order to obtain an image of sufficient quality. An activity ratio of 400:800 MBq might possibly be suitable for such investigations. However, a one-day protocol might then not be feasible for obese patients as there will be too high level of residual rest activity in the rest image.

The aim of this study was therefore to evaluate how the quantification of myocardial perfusion images is influenced by different types of one-day and two-day rest-stress protocols. In order to control the evaluation and be able to create reproducible investigations, we used the Monte Carlo method to simulate SPET projections using a versatile digital phantom and a scintillation camera simulation program. With this technique it is possible to study small changes in specific parameters, in a way that is not possible with repeated patient or physical phantom studies. Also, well-known lesions can be defined in a more flexible way using this technique, than with the physical phantoms available. Two commercially available programs for quantification of myocardial perfusion images were used to assess the different images in an automated and objective way.

Methods

Computer Phantom

We have used the dynamic NURBS-based cardiac-torso (NCAT) phantom throughout this study. This phantom, developed by Segars and colleagues (8), provides a realistic model of the human anatomy and motions of the heart and other organs. The NCAT phantom is a hybrid model offering a combination of the realism of a pixel-based phantom model and the flexibility of a geometry-based phantom model. Flexible models for the various organs and anatomical features that are included in the phantom are based on the visible human male CT data, except for the heart. The heart model is based on a tagged MRI data set (9-11). This phantom makes it possible to define the activity distribution in various organs and to define parameters such as heart size, to specify patient motion (cardiac or respiratory) and anatomic variations. An activity distribution similar to that obtained in a normal myocardial perfusion scintigraphy using $^{99}Tc^{m}$ Sestamibi on a patient was developed based on previously published data (12) and visual inspection of several clinical patient cases. The activity relationship between the right and the left myocardium was determined from measurements in a real patient study. The same procedure was applied to determine the heart/lung activity fraction. The activities in the principal organs within the thorax region are presented in Table 1. A background activity distribution that was close to a corresponding $^{99}Tc^{m}$ Sestamibi distribution was also simulated. The heart size was defined as "normal" according to the NCAT definitions (i.e. 9.49 cm along its major axis and a radius of 2.9 cm (minor axis) resulting in a wall volume of 174 ml).

In our simulations, we assumed the rest images to be the "normal" studies, with a myocardial activity uptake of 7% of the remaining thorax-organs activity. In the stress images, three different types of lesions were defined in the areas supplied by the left anterior descending artery (LAD), the right coronary artery (RCA) and the left circumflex artery (LCx). The lesion volumes were 20, 11.5 and 12 ml, in the LAD, RCA and LCx regions respectively, and corresponded to 11.5%, 7% and 7.1% of the total myocardium, respectively. The Lesion Activity Uptake Reduction (LAUR) relative to the normal myocardial tissue was varied from 20% to 70% in steps of 10%.

Simulation Procedure

The Monte Carlo program SIMIND (13) was used for the simulation of the SPET projections. A typical scintillation camera equipped with a LEHR collimator and a 9.35 mm NaI(Tl) crystal was simulated. The energy resolution was set to 10% FWHM at 140 keV, and the intrinsic spatial resolution was 4.6 mm. SPET projections with a matrix size of 64x64 pixels and a pixel size of 0.63×0.63 cm^2 were simulated for 64 projection angles around 180 degrees in a circular orbit starting at 315 degrees. A 20% energy window centred at the 140 keV photo peak was used. The simulated SPET projections included physical effects such as photon attenuation and contributions from scatter in the phantom, as well as blur due to the limited collimator resolution. The SPET projections were scaled to match the selected stress and rest activities and then added together after first calculating the physical decay of the rest activity corresponding to the time delay between the rest and the stress study. No image noise was added in order to ensure that

small variations in the lesion could be measured. We then compared a one-day rest-stress protocol with a two-day rest-stress protocol. The one-day rest-stress protocol in this study corresponds to an activity ratio of 300:900 MBq with separation times of 0.5, 1, 1.5, 2, 2.5, 3, 3.5 and 4 hours between rest and stress image acquisition. The two-day rest-stress protocol corresponds to an activity ratio of 600:600 MBq with a 24-hour separation time. We also studied the effects of changing the rest-stress activity ratio from 300:900 MBq to 400:800 MBq using a 4-hour separation one-day protocol.

The image set for the heart was created separately from the remaining thorax since the latter activity distribution takes a considerable amount of time to simulate, and will be identical for all simulations of a particular protocol. These two image sets were summed, with suitable normalization (Fig. 1). The initial heart and remaining thorax images were generated from NCAT as gated images corresponding to twenty-four segments. These gated images were then summed to obtain an "ungated" initial perfusion image of the phantom from which the SPET projections were simulated.

Image Reconstruction

Simulated SPET projections were transferred to a clinical image processing station (Philips Pegasys™) and reconstructed with an iterative MLEM algorithm (Philips AutoSPECT™) using twelve iterations; according to our department's clinical procedure. We used a Butterworth post-filter of 5th order with a cut-off frequency of 0.66 cycles/cm for the stress-image reconstructions and 0.55 cycles/cm for rest-image reconstructions. Short-axis images were created by an automatic reorientation procedure albeit the azimuth and the elevation angle were manually adjusted, if necessary, to 33° and 104°, respectively for all reconstructed images since no patient movements were simulated. Typical images are shown in Fig. 2.

Image Evaluation

The short-axis images of the different stress images and the corresponding rest images were analysed using two commercially available programs: the Philips AutoQUANT™ (14) and the 4D-MSPECT program (15). The limits for slice selection of the myocardial base were adjusted manually, maintaining a constant myocardial volume for all evaluations. The ventricular boundary was redefined in order to avoid false contributions to calculation of the extent of the lesion that comes from the myocardial base. If this adjustment is not made, the total extent of the myocardial lesion will be affected by this artefact. The stress and the rest perfusion images were automatically scored regarding radiotracer uptake using the 20 segment model for the left ventricle (16). The segments were scored with a 5-point scoring system (0=normal perfusion; 1=equivocal; 2=moderately reduced; 3=severely reduced; and 4=absent). The Summed Stress Score (SSS), the Summed Rest Score (SRS) and the Summed Difference Score (SDS) were automatically calculated for each study by each software package. The degree of abnormality defined by SSS was classified into four categories: "normal" (SSS=0-3), "mildly abnormal" (SSS=4-8), "moderately abnormal" (SSS=9-13) and "severely abnormal" (SSS>13). In this study, however, the SDS value will equal the SSS value since the SRS values were defined as zero. The measure of the extent (indicating the size of the defect) was also calculated by the two programs.

Results

The variation in the SDS values for the 4-hour separation, one-day protocol and the 24-hour separation, two-day protocol related to LAUR in the three different vascular territories is presented in Fig 3. The scores observed with the two-day protocol were higher than those observed with the one-day protocol. These differences were 3 ± 1 (mean ± SD) for AutoQUANT and 2 ± 1 for 4D-MSPECT. Not only the differences but also the absolute scores were higher for AutoQUANT than for 4D-MSPECT except for the LCx territory.

The corresponding diagrams showing extent instead of SDS values are presented in Fig.4. As with the SDS values, the shift to higher extent values observed with the two-day protocol relative to the one-day protocol occurs over the entire range of LAURs. This shift was 2 ± 1 (mean ± SD) for both AutoQUANT and 4D-MSPECT. This change in extent may not be of clinical importance for deep lesions (high LAUR), since the relative change is small. However, shallow lesions (low LAUR) are proportionally more affected, as shown in Fig. 5. At mid-range values of LAUR, both programs give an extent close to the actual size (11.5%, 7%) when simulating lesions in the LAD and RCA regions, but overestimate the actual size (7.1%) in the LCx region.

The variation in the extent of the LCx lesion depending on separation times between the rest and stress studies ranging from 0.5 the 24 hours is presented in Fig. 6. It can be seen that the calculated size of the extent increases as the separation time increases, which indicates that the residual activity has a measurable impact on the determination of the extent.

The effect of changing activity ratio from 300:900 MBq to 400:800 MBq is presented in Fig. 7. The extent values are lower for the activity ratio of 400:800 MBq and the magnitude of the effect is approximately equivalent to the differences between a two-day and a one-day protocol (Fig. 4).

Discussion

The results presented in this paper show that the residual activity from the rest study will affect the quantification of the stress study and consequently affect the estimation of reversible defects. The differences were found for both AutoQUANT and 4D-MSPECT, in all vascular territories and for defects with low as well as high LAUR. The most serious consequences are likely to appear when stress defects with SDS values just above the limit separating normal and abnormal in the two-day protocol fall below the limit in a one-day protocol situation.

Ideally, a measurement of the extent should reflect its size independently of other factors. However, the results obtained in this study clearly demonstrate that the extent, as given by both AutoQUANT and 4D-MSPECT, depends on both the actual activity uptake in the

lesion relative to the surrounding tissue and the residual myocardial activity from the preceding rest study. This dependence can be understood in terms of an effective spatial resolution and the threshold levels that the programs use in order to determine the extent from the reconstructed images. These dependencies have been described previously (17) but have not been precisely quantified. The method of this paper yields the end-result when commercial packages are applied for SPET evaluation.

It is possible to construct a simple model that provides a link to basic imaging parameters. In this naive model, a lesion in the polar map plot is ideally a well-defined cylindrical well. Because of the limited spatial resolution and cardiac motion, the walls deform into a Gaussian shape (Fig. 8). Depending on the overall spatial resolution, this Gaussian annulus will extend more or less centrally in the well, leaving the inner part intact. Since no counts are lost in the imaging process, but only displaced, the volume of the observed well is equal to that of the original ideal cylindrical well. The size of the lesion is considered to be proportional to the cross-sectional area of the observed well, taken at some threshold. If background activity is present in the imaging process, and if no provision is made to subtract the background in the polar map analysis, this threshold will be counted from the background up, i.e. it will include the background. With the notation of Fig. 8, the threshold condition can be expressed as: $C+b-t = d\times\exp(-\frac{1}{2}(x-r)^2/\sigma^2)$. The ideal lesion size in the polar map representation is πR^2, and the observed lesion size from the polar map is πx^2. Then, the observed size/true size = $x^2 / R^2 = [\sigma\sqrt{(2 \ln[d/(C+b-t)])} + r]^2 / R^2$. The requirement that the lesion volume is unchanged leads to the expression $r = \sigma\times [-\sqrt{(\pi/2)} + \sqrt{(\pi/2 - 2+(R/\sigma)^2)}]$, from which the observed size / true size = $[\sqrt{(2 \ln[d/(C+b-t)])} + \sqrt{(\pi/2-2 + (R/\sigma)^2)} - \sqrt{(\pi/2)}]^2 /(R/\sigma)^2$. This expression is valid when $R/\sigma \geq \sqrt{2}$. For smaller lesions, the observed size / true size = $2 \ln[(R/\sigma)^2 d/(2(C+b-t))]/ (R/\sigma)^2$. These equations have been written to contain R/σ, since this quantity is relevant in an actual measurement. For computational purposes, C (the activity concentration in the myocardial wall above the background activity b) can be set to 100; d to the depth of the well expressed as percentage of C; b to the background activity also expressed as a percentage of C; while t must be expressed relative to C + b: if T is the nominal polar map threshold as a percentage of the maximum, $t = (T/100)(C+b)$, so that the sub-expression (C+b-t) reduces to $(100+b)(1-T/100)$. The model was compared with the Monte Carlo results for the LCx lesion by minimizing the overall sum of the squared deviations for all evaluated separation times between rest and stress studies, and all lesion severities, in a single process. This minimization process regarded the polar map threshold T and R/σ as being free parameters to be fitted. Results from the naive model, fitted to the Monte Carlo simulated data, are shown in Fig. 9. Except for the 20% lesion, the general dependence of the Monte Carlo generated data on background and lesion severity can, thus, be explained by the model.

The two analysis programs show, in general, the same effect with regard to the residual rest activity with only a small disagreement in the calculation of the extent of the same lesion at the same location. This disagreement might be caused by differences in the normal databases used by these programs to determine the stress abnormality. Another explanation of the difference in the calculated extent for the same lesion is that the

programs make use of different definitions of the threshold, a value that forms the base for the definition of the boundary for the lesion.

Conclusions

There are differences in the quantitative assessment of perfusion defects depending on the type of protocol used. The contribution of residual activity is larger when a one-day protocol is used and if a high dose is given at the first examination. The differences could have clinical consequences and result in incorrect image interpretations.

Acknowledgements

The authors would like to thank Edward Ficaro, PhD, University of Michigan Centre for providing details of the 4D-MSPECT program. This work was supported by grants from the Medical Faculty of Lund University, Sweden.

Reference List

(1) Underwood SR, Anagnostopoulos C, Cerqueira M, Ell PJ, Flint EJ, Harbinson M. Myocardial Perfusion Scintigraphy: the evidence. Eur J Nucl Med Mol Imaging 2004; 31:261-291.

(2) Berman DS, Kiat H, Van Train, Germano G, Maddahi J, Friedman JD. Myocardial perfusion imaging with technetium-99m-sestamibi: comparative analysis of available imaging protocols. J Nucl Med 1994; 35:681-688.

(3) Bratt SH, Leclercq B, Itti R, Lahiri A, Sridhara B, Rigo R. Myocardial Imaging with technetium-99m-tetrofosmin: Comparison of one-day and two-day protocols. J Nucl Med 1994; 35:1581-1585.

(4) Montz R, Perez-Castejòn MJ, Jurado JA, Martin-Comin J, Esplugues E, Salgado L et al. Technetium-99m tetrofosmin rest/stress myocardial SPET with a same-day 2-hour protocol: comparison with coronary angiography. Eur J Nucl Med 1996; 23:639-647.

(5) DePuey E, Garcia EV. Updated imaging guidelines for nuclear cardiology procedures, Part 1. J Nucl Cardiol 2001; 8:G1-G58.

(6) Van Train, Garcia EV, Maddahi J, Areeda, J, Cooke CD et al. Multicenter trial validation for quantitative analysis of same-day rest-stress technetium-99m-sestamibi myocardial tomograms. J Nucl Med 1994; 35:609-618.

(7) Radiation Protection 109. Guidance on diagnostic reference levels (DRLs) for medical exposures. European Commission 1999.

(8) Segars WP, Lalush DS, Tsui BMW. A Realistic Spline-Based Dynamic Heart Phantom. IEEE Trans Nucl Sci 1999; 46(3):503-506.

(9) Axel L., R.C.Goncalves, et al. Regional heart wall motion: two-dimensional analysis and functional imaging with MR imaging. Radiology 1992; 183(3):745-750.

(10) Zerhouni E, D.Parish, at al. Human heart: tagging with MR imaging - a method for noninvasive assessment of myocardial function. Radiology 1988; 169:59-63.

(11) McVeigh E, E.Atalar. Cardiac tagging with breath hold CINE MRI. Magn Reson Med 1992; 28:318-327.

(12) Wackers FJ, Berman DS, Maddahi J, et al. Technetium-99m hexakis 2-methoxyisobutyl isonitrile: Human biodistribution, dosimetry, safety, and preliminary comparison to thallium-201 for myocardial perfusion imaging. J Nucl Med 1989; 30:301-311.

(13) Ljungberg M, Strand S-E. A Monte Carlo Program Simulating Scintillation Camera Imaging. Comp Meth Progr Biomed 1989; 29:257-272.

(14) AutoQuant. AutoQUANT 4.3.1, Philips user manual 9201-0225D-ENG, REV A. 1999.

(15) The Regents of the University of Michigan. The Users Manual for 4D-MSPECT. 2003.

(16) Guido Germano, Daniel S.Berman. An Approach to the Interpretation and reporting of gated Myocardial Perfusion SPECT. 1999;(5):155-158.

(17) RL Eisner, RE Patterson. The challenge of quantifying defect size and severity: Reality versus algorithm. J Nucl Cardiol 1999; 6:36-71.

Table1.
The relative activity concentration in each organ used in the NCAT study.

Organ	Relative activity concentration
LV myocardium	100
RV myocardium	60
Liver	40
Lungs	5
Gall bladder	250
Kidneys	140
Spleen	22
Stomach	3
Remaining thorax	2

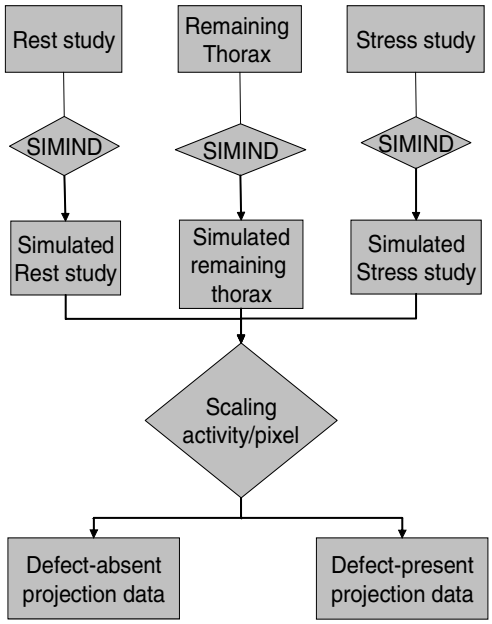
Rest study
Remaining Thorax
Stress study
SIMIND
SIMIND
SIMIND
Simulated Rest study
Simulated remaining thorax
Simulated Stress study
Scaling activity/pixel
Defect-absent projection data
Defect-present projection data

Fig. 1.

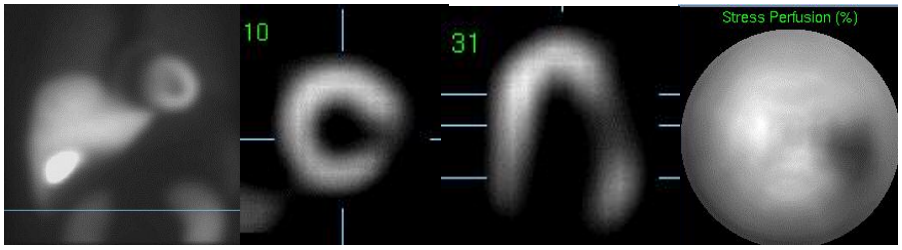

a) **b)** **c)** **d)**

Fig. 2.

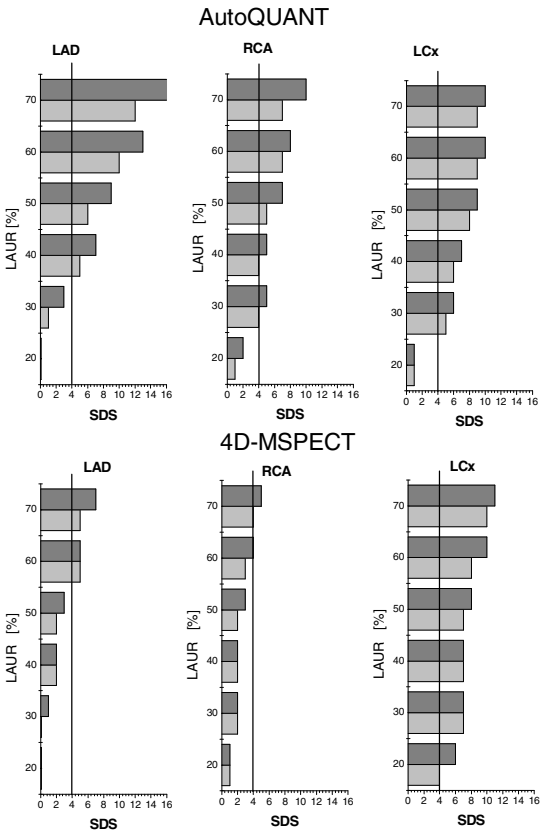

Fig. 3.

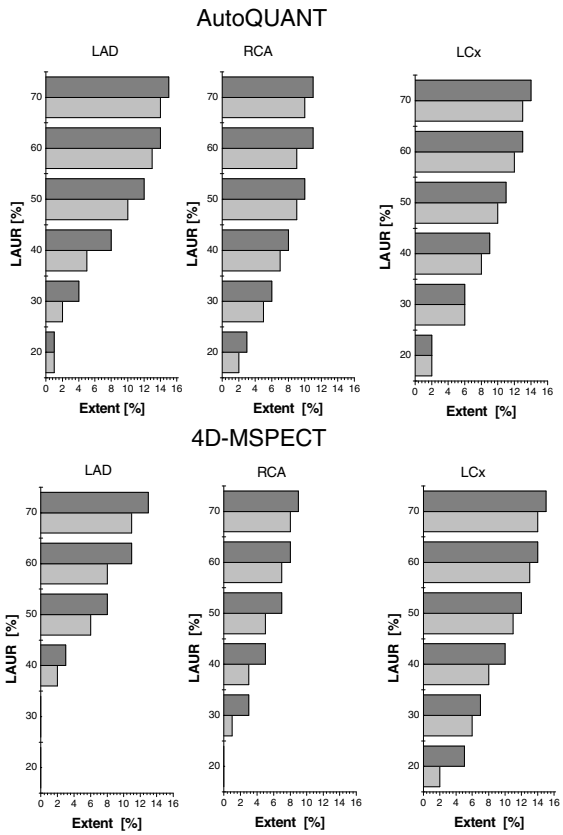
AutoQUANT
LAD
RCA
LCx
LAUR [%]
Extent [%]
4D-MSPECT
LAD
RCA
LCx
LAUR [%]
Extent [%]

Fig. 4.

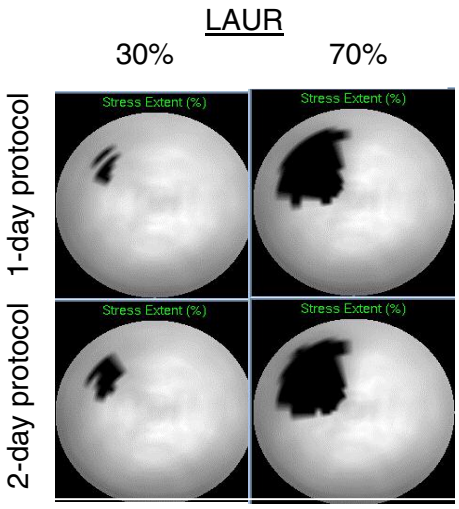
LAUR
30%
70%
1-day protocol
2-day protocol
Stress Extent (%)
Stress Extent (%)
Stress Extent (%)
Stress Extent (%)

Fig. 5.

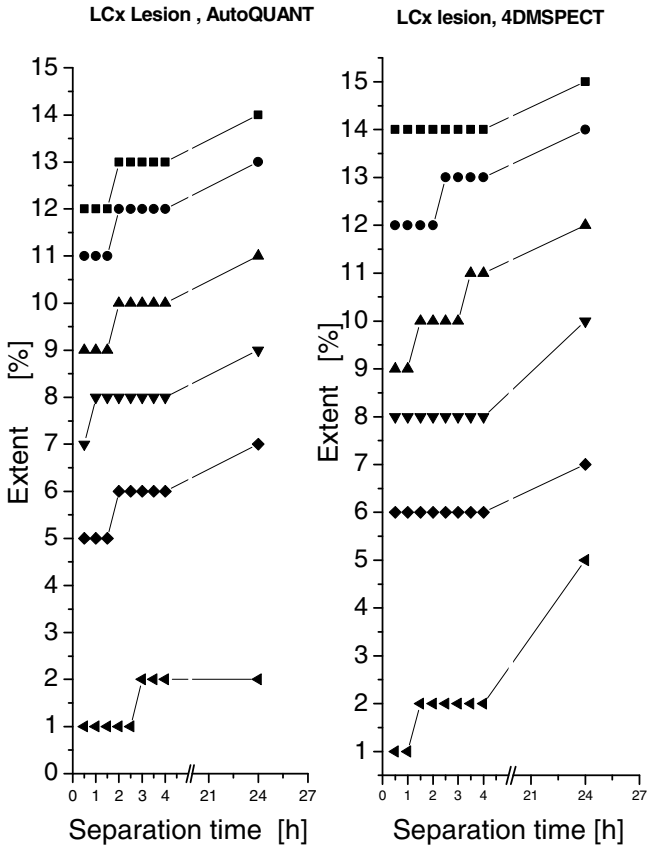
LCx Lesion , AutoQUANT
LCx lesion, 4DMSPECT
Extent [%]
Separation time [h]
0 1 2 3 4 21 24 27

Fig. 6.

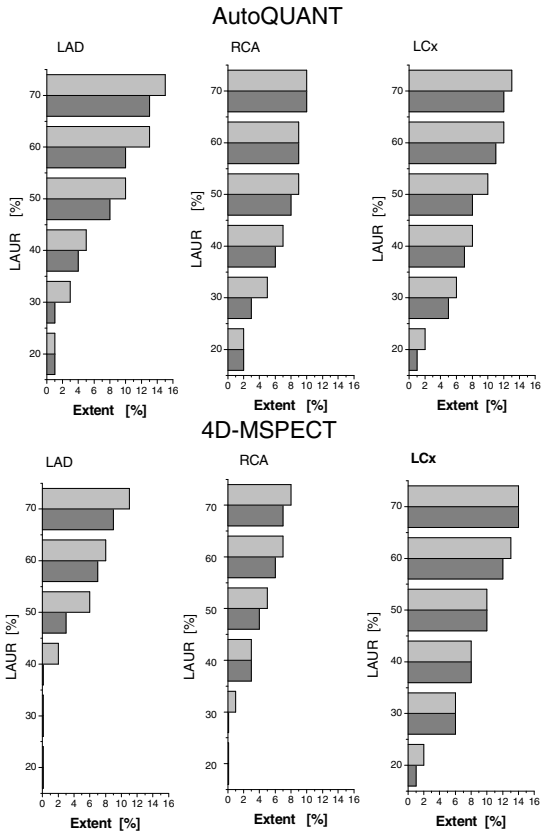
AutoQUANT
LAD
RCA
LCx
LAUR [%]
Extent [%]
4D-MSPECT
LAD
RCA
LCx
LAUR [%]
Extent [%]

Fig.7.

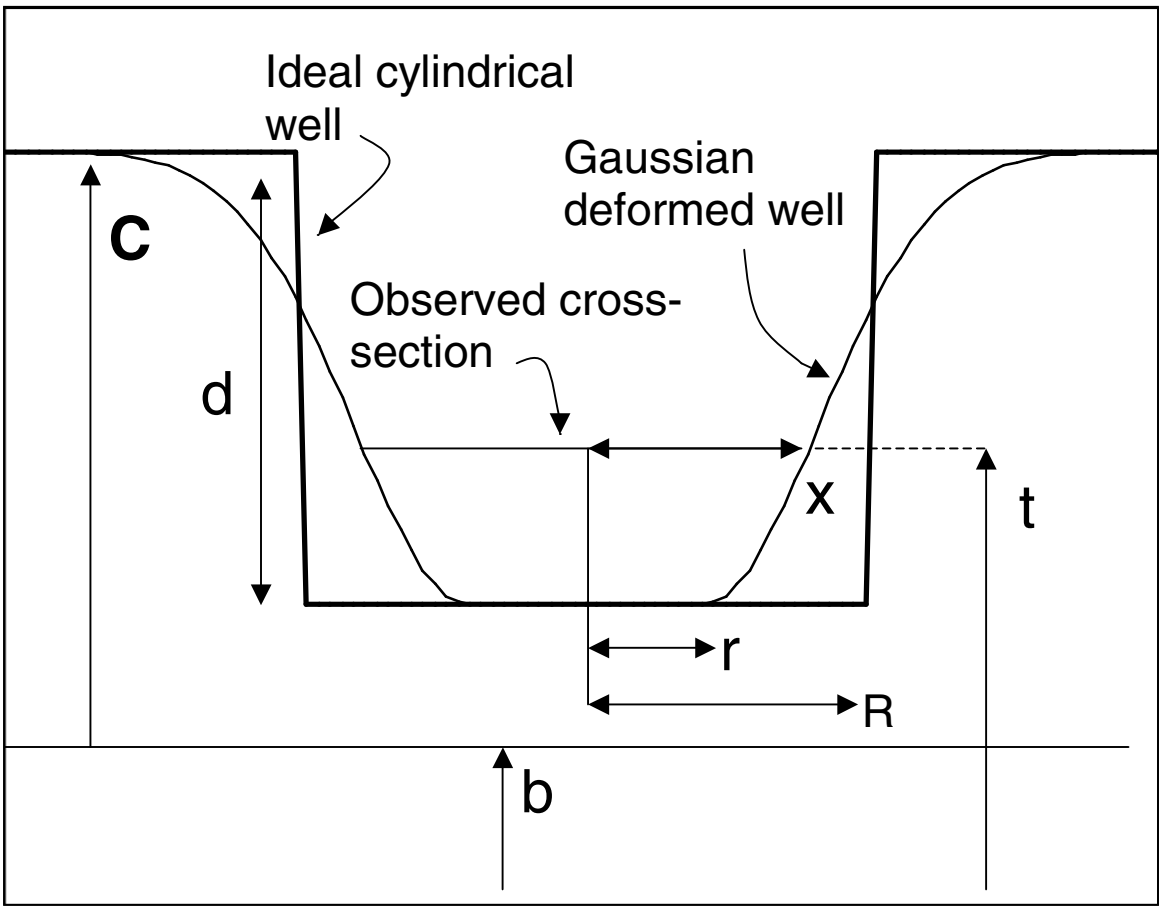
Ideal cylindrical
well
Gaussian
deformed well
c
Observed cross-
section
d
x
t
r
R
b

Fig. 8.

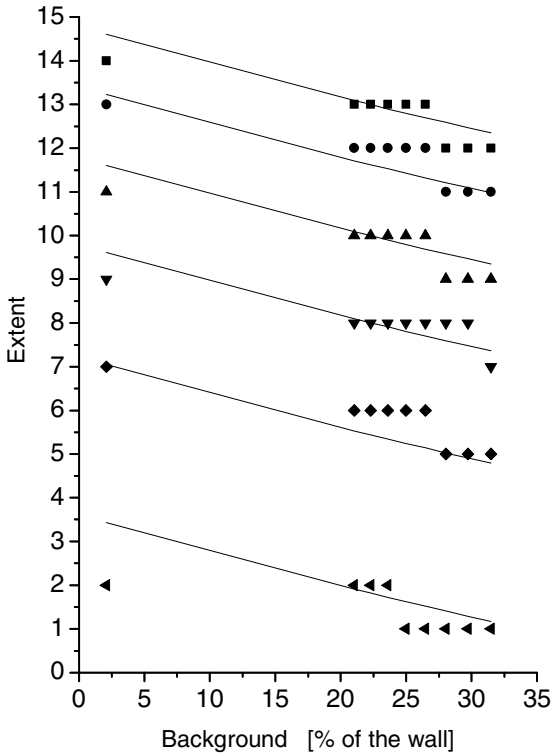
Extent
Background [% of the wall]
0
1
2
3
4
5
6
7
8
9
10
11
12
13
14
15
0
5
10
15
20
25
30
35

Fig. 9.

Figure legends

Fig. 1. A flow-chart describing the procedure for the generation of lesion-present and lesion-absent data for our study. The SPET projections for the background activity distribution in the other organs are simulated separately and summed to form the final SPET projection.

Fig. 2. An example of simulated defected heart images from the NCAT showing: a) a SPET projection, b) a reconstructed short-axis image, c) a vertical long axis image and d) the polar map.

Fig. 3. Calculated SDS values for the 4-hour, one-day protocol (light grey bars) and for the 24-hour two-day protocol (dark grey bars). The vertical solid lines show the limit for SDS values defined as abnormal.

Fig. 4. The variation in the calculated extent of the lesion as a function of the LAUR for the 4-hour, one-day protocol and for the 24-hour, two-day protocol.

Fig. 5. The upper pair of images shows polar maps for lesions in the LAD region with 30% and 70% LAURs obtained with the 4-hour, one-day protocol. The lower pair of images shows equivalent data from the two-day protocol.

Fig. 6. Variation in the calculated extent of the lesion for LAURs of 70% (■), 60% (●), 50% (▲), 40% (▼), 30% (◆) and 20% (◀) for different times between the rest and the stress studies. Discrete jumps are caused by integer number representation from the programs.

Fig. 7. Calculated values of the extent of the lesion for a 4-hour, one-day study with rest:stress activity ratios of 300:900 (light grey bars) and 400:800 (dark grey bars) respectively.

Fig. 8. The parameters used to define the naive model. The walls of the lesion, ideally cylindrical, are deformed into a Gaussian-shaped annulus due to the limited spatial resolution of the SPET system and by cardiac motion. For a specific threshold, t, the observed lesion size is proportional to πx^2. C is the activity concentration in the myocardial wall above the background activity b; d is the depth of the well; R the radius of the ideal lesion and r the radius of the intact inner part of the observed lesion.

Fig. 9. Results from the naive model (solid lines) fitted to Monte-Carlo simulated results for LCx located lesions. The LAURs are; (■) 70 %, (●) 60%, (▲) 50 %, (▼) 40 %, (◆) 30 % and (◀) 20% of the normal uptake.